Formation of carbon vacancy in 4H silicon carbide during high-temperature processing

H. M. Ayedh, , V. Bobal, , R. Nipoti, , A. Hallén, and , and B. G. Svensson

Citation: Journal of Applied Physics **115**, 012005 (2014); doi: 10.1063/1.4837996
View online: http://dx.doi.org/10.1063/1.4837996
View Table of Contents: http://aip.scitation.org/toc/jap/115/1
Published by the American Institute of Physics

Formation of carbon vacancy in 4H silicon carbide during high-temperature processing

H. M. Ayedh,[1] V. Bobal,[1] R. Nipoti,[2] A. Hallén,[3] and B. G. Svensson[1]
[1]*Department of Physics/Center for Materials Science and Nanotechnology, University of Oslo, P.O. Box 1048 Blindern, N-0316 Oslo, Norway*
[2]*Consiglio Nazionale delle Ricerche, Istituto di Microelettronica e Microsistemi, Sezione di Bologna (CNR-IMM of Bologna), via Gobetti 101, I-40129 Bologna, Italy*
[3]*Royal Institute of Technology, School of Information and Communication Technology (ICT), SE-164 40 Kista-Stcokholm, Sweden*

(Received 15 September 2013; accepted 24 October 2013; published online 2 January 2014)

As-grown and pre-oxidized silicon carbide (SiC) samples of polytype 4H have been annealed at temperatures up to 1950 °C for 10 min duration using inductive heating, or at 2000 °C for 30 s using microwave heating. The samples consisted of a n-type high-purity epitaxial layer grown on 4° off-axis ⟨0001⟩ n^+-substrate and the evolution of the carbon vacancy (V_C) concentration in the epitaxial layer was monitored by deep level transient spectroscopy via the characteristic $Z_{1/2}$ peak. $Z_{1/2}$ appears at ∼0.7 eV below the conduction band edge and arises from the doubly negative charge state of V_C. The concentration of V_C increases strongly after treatment at temperatures ≥ 1600 °C and it reaches almost 10^{15} cm^{-3} after the inductive heating at 1950 °C. A formation enthalpy of ∼5.0 eV is deduced for V_C, in close agreement with recent theoretical predictions in the literature, and the entropy factor is found to be ∼5 k (k denotes Boltzmann's constant). The latter value indicates substantial lattice relaxation around V_C, consistent with V_C being a negative-U system exhibiting considerable Jahn-Teller distortion. The microwave heated samples show evidence of non-equilibrium conditions due to the short duration used and display a lower content of V_C than the inductively heated ones. Finally, concentration-versus-depth profiles of V_C favour formation in the "bulk" of the epitaxial layer as the prevailing process and not a Schottky type process at the surface. © *2014 AIP Publishing LLC*. [http://dx.doi.org/10.1063/1.4837996]

I. INTRODUCTION

Silicon carbide (SiC) is a wide bandgap semiconductor material with more than 200 different polytypes reported in the literature of which the most commonly studies ones are 4H-SiC, 6H-SiC, and 3C-SiC. The material quality of SiC has been gradually improved during the past ∼20 years utilizing novel techniques like chemical vapor deposition (CVD) for growth of high-purity epitaxial layers on bulk SiC substrates.[1] These layers are worthy for realization of advanced power electronic devices operating at high voltage, high temperature, and high frequency and exploiting the full potential of the attractive inherent properties of SiC. This holds especially for the 4H polytype where wafers with diameter of 6 in. are becoming commercially available.

A fundamental limit of a semiconductors electrical performance is the presence of intrinsic point defects acting as traps and/or recombination centers for charge carriers; in 4H-SiC, the dominant electrically active defects are the so-called $Z_{1/2}$ and EH_7 centers. $Z_{1/2}$ and EH_7 occur with a typical concentration in the 10^{12}–10^{13} cm^{-3} range in as-grown epitaxial layers and are enhanced by irradiation with energetic electrons and ions[2–6] but suppressed by thermal oxidation of the layer surface.[7,8] Further, both centers display a high thermal stability, persisting up to 2000 °C after electron irradiation,[9] and they can even start to increase in concentration at sufficiently high temperature.[10]

The $Z_{1/2}$ center is known to exhibit negative-U character,[6] and the identity of $Z_{1/2}$ and EH_7 have been a long-lasting issue in the literature. However, in a recent study Son *et al.*[11] used electron paramagnetic resonance (EPR) measurements together with photo-excitation to determine the energy levels of the carbon vacancy (V_C) and to study its negative-U properties, and combining these results with those from deep level transient spectroscopy (DLTS), $Z_{1/2}$ and EH_7 were firmly identified as different charge states of V_C. We will adopt this identification and unambiguously show that $Z_{1/2}$ originates from a double-acceptor state ($V_C(2-/0)$; V_C is neutral when the state is empty and doubly negatively charged when filled) and EH_7 from a single donor state ($V_C(0/+)$). Moreover, the evolution of [V_C] (brackets denote concentration) during high-temperature treatment will be studied by monitoring the $Z_{1/2}$ peak using DLTS.

Device processing using 4H-SiC wafers requires typically temperatures in excess of ∼1600 °C and this is especially true for selective area doping where ion implantation is the prevailing technique.[12,13] In particular, p-type doping is demanding since suitable group-III elements, like B and Al, display rather deep acceptor levels in the bandgap with positions of ∼0.15 to ∼0.30 eV above the valence band edge (E_V)[12–15] and they have also a limited solid solubility in the low 10^{20} cm^{-3} range.[16] Despite a higher defect generation, because of its heavier mass, Al is generally the preferred element since its acceptor states are more shallow and diffusion is less during post-implantation annealing than for B.[15,17] Hence, in order to realize low-resistivity p-type layers required for efficient bipolar power devices, the trend has been to increase the implanted Al content per unit volume

and to increase the post-implant annealing temperature, the former up to the low $10^{21}\,cm^{-3}$ range and the latter up to 1800 °C.[14,15] Recently, a state-of-the-art p-type resistivity in the low 10^{-2} Ωcm range, at room temperature (RT), was reported using a content of 8×10^{20} Al/cm^3 and microwave furnace annealing (MWA) at ≥2000 °C for 30 s.[13] Similar results were also very recently obtained employing more conventional annealing (CA) in an inductively heated furnace at 1950 °C for 5 min.[12]

On the other hand, high-temperature processing of 4H-SiC may have an adverse effect on the concentration of intrinsic point defects and this concerns particularly V_C, which is a prime life-time-controlling defect through its $Z_{1/2}$ state.[18] In this study, we show that $[V_C]$ is, indeed, enhanced by CA above 1600 °C whilst the effect is somewhat less pronounced for MWA, reflecting non-equilibrium conditions in the latter case. Further, the formation enthalpy is determined for V_C, showing excellent agreement with recent theoretical predictions in the literature, and a bulk mechanism appears to dominate the formation process rather than a surface (Schottky) one.

II. EXPERIMENTAL

N-type (nitrogen doped) 4H-SiC wafers were purchased from Cree Inc. and consisted of a CVD-grown epitaxial layer with a thickness of ∼10 μm on Si-face highly doped bulk substrate (bulk net carrier concentration $\sim 10^{18}\,cm^{-3}$). The growth direction was 4° off the c-axis and the epitaxial layer had a net carrier concentration of $\sim 2.4 \times 10^{15}$ cm^{-3}, as determined by capacitance-voltage (CV) measurements. The wafers were cut into samples with a size of 5×7 mm^2, and these samples were divided into three groups (A, B, and C).

The group A samples were implanted at RT by 4.3 MeV ^{28}Si ions to fluences between (1-4) $\times 10^8$ cm^{-2}. The implants were performed in a direction close to the sample normal in order to suppress channelling effects.[19] Subsequently, annealing was undertaken at 1150 °C for 3.5 h in flowing nitrogen atmosphere to reduce the concentration of other defects less stable than V_C.[5]

The group B samples were protected by a pyrolyzed resist film (C-cap) after native oxide etching, where the resist pyrolysis took place in forming gas at 900 °C for 2 min. Then, isochronal heat treatment (10 min) was performed at 1600, 1800, and 1950 °C in high purity Ar ambient by using an inductively heated furnace where the samples were hosted in a graphite box with glassy carbon coated surfaces. During this so-called CA, an optical pyrometer reads the temperature of the sample holder, and the treatment features a heating rate of 40 °C/s and an almost exponential cooling with about 50 s time constant. The temperature overshoot is ≤15 °C with a duration of ≤20 s. In addition, one sample was annealed at 2000 °C for 30 s in a microwave heated system[20] having forming gas ambient. In this MWA system, a cup of refractory material hosts the sample and an optical pyrometer reads the sample temperature, featuring a ∼200 °C/s heating ramp and an almost exponential cooling with about 20 s time constant, and a null temperature overshoot.

The group C samples were first annealed in dry O_2 atmosphere at 1150 °C for 6.5 h yielding a ∼700 Å thick layer of SiO_2. After removal of the SiO_2 layer in diluted hydrofluoric (HF) acid, the group C samples were identically treated as the group B ones, i.e., the two sets of samples were pyrolyzed and annealed together at all the temperatures employed (1600, 1800, 1950, and 2000 °C).

After a standard cleaning procedure, circular Schottky barrier (SB) diodes were formed by electron beam evaporation of nickel through a shadow mask at a base pressure of $\sim 2 \times 10^{-7}$ Torr. As Ohmic back-side contact, coating with silver paste was used. Characterization of the samples was performed by CV-profiling and DLTS using an upgraded version of the setup described in Ref. 21, equipped with a HP4280A capacitance meter and a high temperature cryostat. The measurements were conducted at sample temperatures from 50 K to 700 K. For the CV scans, a probe (oscillating) voltage $\Delta V_{osc} = 30$ mV with a frequency $\omega_{osc} = 1$ MHz was used together with a voltage increment $\Delta V_{step} = 500$ mV and sweep rate $\omega_{step} = 1$ Hz for the reverse bias voltage. For DLTS, six spectra with rate windows between $(100\,ms)^{-1}$ and $(3200\,ms)^{-1}$ (or $(20\,ms)^{-1}$ and $(640\,ms)^{-1}$) were acquired simultaneously during one temperature scan. The quiescent reverse bias voltage applied ranged from −5 V to −14 V with a corresponding filling pulse voltage of +5 V to +14 V such that defect levels were monitored at depths ranging from ∼0.5 μm to ∼3.0 μm. The filling pulse duration was 50 ms to ensure saturation trapping of the $Z_{1/2}$ and EH_7 levels. Concentration-versus-depth profiles of $Z_{1/2}$ and EH_7 were obtained by selecting one rate window and holding the temperature constant at the maximum of the studied peak. The steady-state reverse bias voltage was kept constant while gradually increasing the amplitude of the filling pulse. The depth profile was then extracted from the dependence of the recorded signal on the pulse amplitude, where the voltages used were converted into depth according to the conventional relations for a SB diode and accounting for the so-called λ-effect.

III. RESULTS AND DISCUSSION

A. Charge state transitions of V_C; $Z_{1/2}$ and EH_7

Figure 1 shows DLTS spectra of an as grown sample and one group A sample implanted with a fluence of 3×10^8 Si^+/cm^2 and then annealed at 1150 °C (3.5 h). Both spectra are dominated by the $Z_{1/2}$ and $EH_{(6/7)}$ peaks while other peaks are of minor importance having more than one order of magnitude lower intensity. $Z_{1/2}$ and $EH_{(6/7)}$ are located at ∼0.70 eV and ∼1.5 eV below the conduction band edge (E_C), respectively, where $EH_{(6/7)}$ is somewhat broad with two contributions, EH_6 and EH_7. High-energy resolution studies, including Laplace transform DLTS,[22–25] have shown that EH_7 prevails over EH_6 by a factor of typically 3 to 4, and in the following we will refer to EH_7 only. In the implanted/annealed sample, $Z_{1/2}$ and EH_7 are enhanced by a factor of almost 40 relative to the as grown sample which has a uniform concentration of $Z_{1/2}$ and EH_7 of $\sim 4 \times 10^{12}$ cm^{-3} (accounting for that the $Z_{1/2}$ peak is due to emission of two electrons). Within the experimental accuracy, the amplitudes of $Z_{1/2}$ and EH_7 increase linearly with ion fluence in the studied range, and for fluences $\geq 1 \times 10^8$ cm^{-2} the background

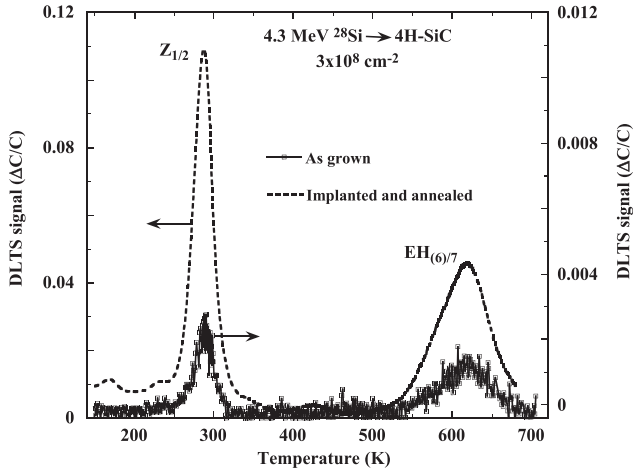

FIG. 1. DLTS spectra of an as grown sample and one group A sample implanted with 4.3 MeV Si ions to a fluence of 3×10^8 cm^{-2} and then annealed at 1150 °C in flowing nitrogen. The spectra are dominated by the $Z_{1/2}$ peak at $\sim E_C - 0.70$ eV and the EH_7 peak at $\sim E_C - 1.5$ eV (rate window = (3200 ms)$^{-1}$).

concentration of $Z_{1/2}$ and EH_7 can be neglected. The generation rate of $Z_{1/2}$ and EH_7 at the peak of the defect-versus-depth profile is ~4% of that of V_C, as estimated by comparison with Monte Carlo calculations of the implantation-induced defect distribution using the TRIM-code (SRIM version 2006.02)[26] and energy threshold values of 20 and 35 eV for the displacement of C and Si, respectively. Effects of dynamic annealing are omitted in the calculations and the generation rate value of ~4% is in the range anticipated for a fundamental (first-order) defect like V_C.[27]

In Fig. 2, experimental and numerically simulated carrier concentration profiles obtained at 190, 300, and 645 K are compared for an implanted/annealed group A sample subjected to a fluence of 4×10^8 cm^{-2}. In the simulations, only $Z_{1/2}$ and EH_7 are accounted for whereas the contribution from other defects is neglected since they exhibit more than one order of magnitude lower concentration, see Fig. 1. The

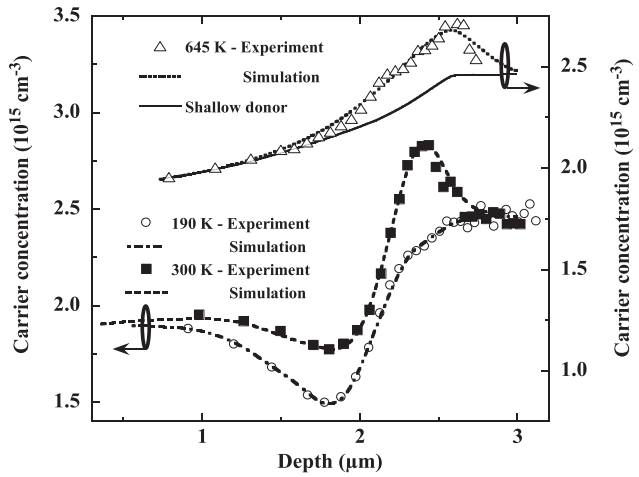

FIG. 2. Comparison between measured and simulated carrier concentration profiles at temperatures of 190, 300, and 645 K for a group A sample implanted with an ion fluence of 4×10^8 cm^{-2}. In the simulations, $Z_{1/2}$ and EH_7 are ascribed to a double acceptor and a single donor, respectively.

simulations utilize a refined version of the model originally developed by Kimerling in Ref. 28 and details are provided elsewhere.[29] At 190 K, the emission rate of electrons from $Z_{1/2}$, $e_n(Z_{1/2})$, is negligible compared to both ω_{osc} and ω_{step}, and the recorded data yield the true profile of responding electrons, i.e., the difference between the profile of shallow (effective) nitrogen donors and that of electrons trapped by $Z_{1/2}$. At 300 K, $\omega_{step} < e_n(Z_{1/2}) < \omega_{osc}$ and an anomalous peak occurs at ~2.4 μm. The appearance of such a peak is a unique feature of deep acceptor-like traps with non-uniform depth distribution.[28] No evidence is found for a donor-like behaviour of $Z_{1/2}$, as originally suggested by Hemmingsson *et al.*[6] Further, at 645 K $e_n(Z_{1/2})$ exceeds both ω_{step} and ω_{osc} and the data at this temperature unambiguously rule out $Z_{1/2}$ as a donor since the electron concentration at the maximum position of the implantation-induced defect profile (~1.8 μm) is essentially equal to the effective concentration of shallow nitrogen donors. Moreover, EH_7 starts to respond above ~500 K and the intermediate case of $\omega_{step} < e_n(EH_7) < \omega_{osc}$ holds at 645 K; the peak emerging at large depth (~2.6 μm), together with no loss of conduction electrons at the defect profile peak (~1.8 μm), is an unambiguous evidence for the donor nature of EH_7.[28,29] Indeed, as illustrated in Fig. 2, the experimental data at the three different temperatures are all closely reproduced by treating $Z_{1/2}$ as a double acceptor and EH_7 as a single donor in the simulations. In addition, $Z_{1/2}$ and EH_7 exhibit identical concentration-versus-depth profiles except for a two-to-one ratio, consistent with their double acceptor and single donor character. Hence, these data corroborate fully the identification of $Z_{1/2}$ and EH_7 as $V_C(2-/0)$ and $V_C(0/+)$, respectively, made in Ref. 11. In the following Sec. III B, the $Z_{1/2}$ peak will be utilized to monitor the evolution of V_C during CA and MWA of the group B and C samples.

B. Thermal formation of V_C

Figure 3 shows DLTS spectra from 90 to 350 K of the group B and C samples undergone CA at 1950 °C, together with the spectra of the corresponding control samples. In all the samples, the $V_C(2-/0)$ (or $Z_{1/2}$) peak dominates and the amplitude is drastically enhanced by a factor of ~30 and ~200 in the group B and group C samples, respectively, after the heat treatment. The resulting concentration of trapped/emitted electrons by V_C exceeds 20% of the dopant concentration, and a close inspection of the spectra in Fig. 3 unveils a shift in the peak position by ~5–7 K towards low temperatures in the annealed samples compared to the control ones. At such high relative trap concentrations, which are not fully ideal for detailed DLTS analysis, the peak broadens and shifts towards low temperatures because of carrier freeze out, as discussed in Ref. 30. The stronger relative increase of $[V_C]$ in the group C samples is due to a lower initial concentration whilst the absolute peak amplitudes after the annealing are almost identical. Thermal oxidation of the Si face at comparatively modest temperatures (~1100 °C) has recently been shown to reduce the concentration of V_C ($Z_{1/2}$) by orders of magnitude,[7,8] and effectively, a deep "free of V_C" layer forms extending several tens of μm into the sample.

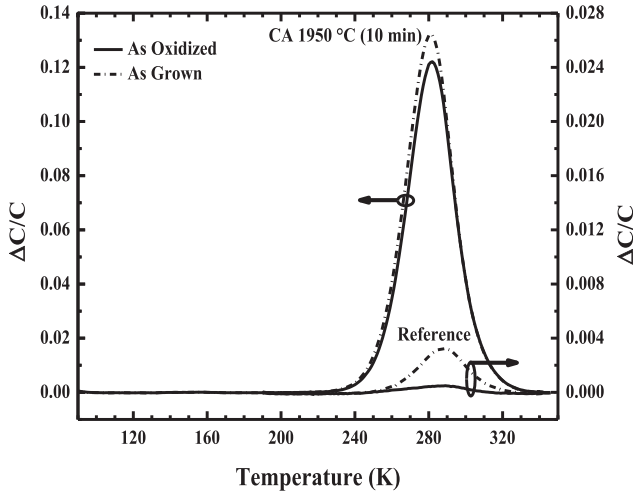

FIG. 3. DLTS spectra of as grown (group B) and as oxidized (group C) samples subjected to CA at 1950 °C. Spectra of the corresponding control (reference) samples are also included for comparison. The $V_C(2-/0)$ peak (or $Z_{1/2}$) is strongly predominant in the studied temperature range (90–350 K) (rate window = $(640\,\text{ms})^{-1}$).

The reduction in $[V_C]$ is attributed to injection of interstitial carbon atoms (C_I's) from the SiO_2/SiC interface and subsequent annihilation of V_C. The fact that $[V_C]$ is essentially identical in the group B and C samples after the 1950 °C annealing, despite the large difference in initial concentration, implies that steady-state conditions are reached where formation (and not annihilation/annealing of V_C's persisting after growth) prevails. In Fig. 4, data for the amplitude of the $V_C(2-/0)$ peak versus annealing temperature are displayed for all the group B and C samples subjected to CA. V_C grows rapidly between 1600 and 1950 °C, especially in the group C samples because of their low initial concentration. Below 1600 °C, the increase is small and in particular, this is true for the group B samples where $[V_C]$ remains almost constant relative to the control sample. However, in absolute values the DLTS signal (ΔC/C) increases by $\sim 1 \times 10^{-3}$ in the B sample at 1600 °C which is close to the total signal in the C sample. This indicates that the formation rate of V_C dominates also at 1600 °C compared to the rate of annealing/annihilation of the V_C's present after growth; hence, the latter rate is slow and the signal in the B samples after the 1600 °C treatment does not reflect steady-state (or equilibrium) conditions which are more appropriately represented by the signal in the C samples. After 1800 °C (and 1950 °C), the B and C samples yield identical values, within the experimental accuracy, and steady-state conditions can be assumed for both groups of samples.

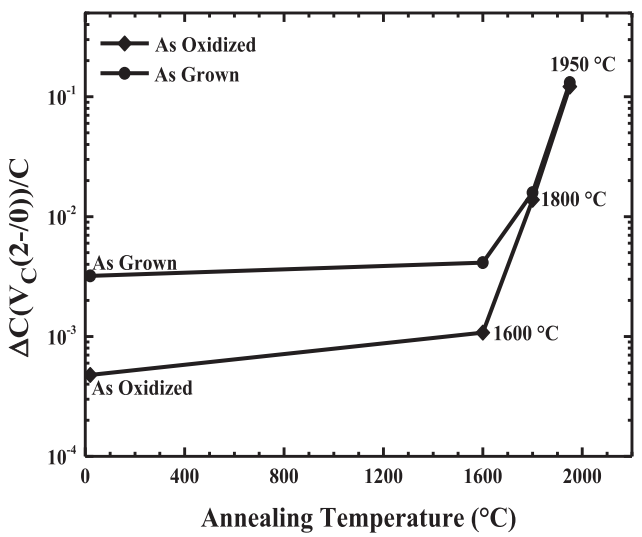

FIG. 4. Amplitude of the $V_C(2-/0)$ peak as a function of annealing temperature for the as grown (group B) and as oxidized (group C) samples subjected to CA.

In Fig. 5, the amplitude of the $V_C(2-/0)$ peak is depicted versus the reciprocal absolute annealing temperature for the group B and C samples subjected to CA. The data obey an Arrhenius behaviour with a high degree of correlation (correlation coefficient > 0.9978) and an energy of ~5.0 eV is deduced for the formation of V_C assuming the following relation:

$$[V_C] = N_{C-sites} exp\left(-\frac{E_{Form}}{kT}\right), \quad (1)$$

where $N_{C-sites}$ is the concentration of available C sites in the SiC lattice, E_{Form} is the formation energy of V_C, k is Boltzmann's constant and T is the absolute annealing temperature. In the data analysis, the value measured for the group B sample at 1600 °C is omitted as it does not represent steady-state conditions, as discussed above. Equation (1) is valid in the dilute limit,[31] which applies since $[V_C] \leq 10^{15}\,\text{cm}^{-3}$ and $N_{C-sites} \cong 10^{23}\,\text{cm}^{-3}$. The pre-exponential factor extracted from the data in Fig. 5 is on the order of $10^{25}\,\text{cm}^{-3}$, with an uncertainty of less than one order of magnitude. The accuracy of the $[V_C]$ data is ~10% and the value deduced for E_{Form} is estimated to be valid within less than ±0.2 eV. The value obtained for the pre-exponential factor exceeds $N_{C-sites}$ by more than two orders of magnitude and

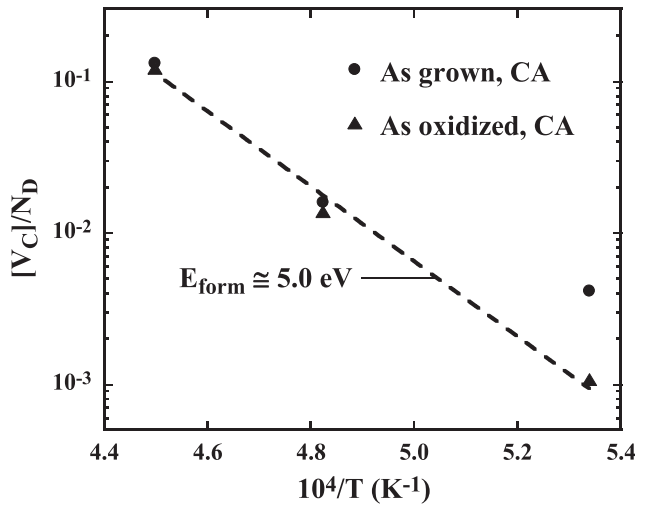

FIG. 5. The carbon vacancy concentration normalized to the dopant concentration versus the reciprocal absolute annealing temperature for the as grown (group B) and as oxidized (group C) samples subjected to CA. Omitting the value for the group B sample at 1600 °C, as outlined in the text, a formation enthalpy of V_C of ~5.0 eV is extracted from the slope of the data (correlation coefficient > 0.9978).

TABLE I. Survey of the amplitudes of the $V_C(2-/0)$ peak in the group B and C samples after CA and MWA.

Sample	Heat treatment	$\Delta C(V_C(2-/0))/C$
As grown (Group B)	…	0.0032
	CA: 1600 °C	0.0041
	CA: 1800 °C	0.0158
	CA: 1950 °C	0.1313
	MWA: 2000 °C	0.0719
As oxidized (Group C)	…	0.0005
	CA: 1600 °C	0.0011
	CA: 1800 °C	0.0138
	CA: 1950 °C	0.1215
	MWA: 2000 °C	0.0485

this may indicate a considerable increase of the crystal entropy, ΔS, during V_C formation. In Eq. (1), ΔS is not accounted for and it enters as a factor $exp\left(\frac{\Delta S}{k}\right)$ in the pre-exponent (and E_{Form} represents now the enthalpy of formation). Assuming $N_{C-sites} \cong 5 \times 10^{22}$ cm^{-3}, one obtains $\Delta S \approx 5k$ which is rather substantial and implies that atomic re-arrangement occurs around V_C. Indeed, this is expected since the negative-U behaviour of V_C shows that the defect is prone to large lattice relaxation; the dangling bonds of the surrounding Si atoms have an extended character leading to formation of re-constructed bonds giving rise to symmetry lowering and considerable Jahn-Teller distortion of V_C.[32,33] In contrast, for V_{Si} no such distortion is predicted since the dangling bonds of the surrounding C atoms are strongly localized and instead formation of a non-degenerate high-spin state dominates.[34]

During the CA (as well as during the MWA), carbon-rich conditions are anticipated because of the C-cap used and hosting of the samples in a graphite box; for such conditions calculations based on density-functional-theory employing the local-density approximation for the exchange-correlation functional predict a formation energy of V_C in 4H-SiC of ~4.4–4.5 eV.[32,33] This is slightly lower than the value extracted in Fig. 5 but recent large scale and gap error free calculations utilizing the Heyd-Scuseria-Ernserhof hybrid functional (HSE06) give a value of ~5.0 eV,[35] which is identical to our experimental one. Here, it should also be mentioned that Zippelius *et al.*[10] have reported a somewhat higher experimental value of 5.7–6.6 eV for E_{Form} but the data in Ref. 10 were of preliminary character.[36]

In Table I, the amplitudes of the $V_C(2-/0)$ peak in the CA samples are compared with those in the samples treated by MWA. Despite the higher temperature, the latter ones exhibit lower concentration of V_C than the former ones annealed at 1950 °C, which is presumably due to non-equilibrium conditions during the MWA with a duration of only 30 s. Extrapolation of the data in Fig. 5 to an annealing temperature of 2000 °C gives $[V_C]$ values about a factor of 4–5 higher than those reached in the MWA samples. This suppressed formation of V_C for MWA translates into a corresponding longer minority carrier life-time,[18] which is highly desirable for optimum performance of bipolar SiC devices. Thus, considering that MWA at temperatures $\geq$ 2000 °C yield similar (or superior) electrical activation of high-fluence Al-implanted layers as CA at 1950 °C, reaching a resistivity at RT in the low 10^{-2} Ω cm range,[12,13] MWA may perhaps be regarded as superior to CA in conjunction with heavy p^+-doping by ion implantation.

However, no definite conclusion on the use of MWA versus CA can be made at this stage and further understanding of the mechanism(s) of V_C formation needs to be acquired. We have, therefore, also undertaken concentration-versus-depth measurements of V_C and the results are depicted in Figs. 6(a) and 6(b) for samples undergone CA and MWA, respectively. For clarity, in Fig. 6(a) only the results for the group B samples are included since the group C samples display identical behaviour (except for lower absolute values after the 1600 °C anneal). In the as grown state as well as after oxidation, V_C exhibits a uniform distribution in the studied depth interval (~0.6 to ~1.8 μm) and the same holds after CA at 1600 °C. In contrast, the 1800 °C profile indicates a small increase with depth and this trend is strongly enhanced in the 1950 °C sample where $[V_C]$ increases by almost a factor of two between 0.6 and 1.8 μm. Also the MWA samples show an increase of $[V_C]$ with depth, Fig. 6(b), although substantially weaker than for the CA ones at 1950 °C. These data favour V_C formation in the

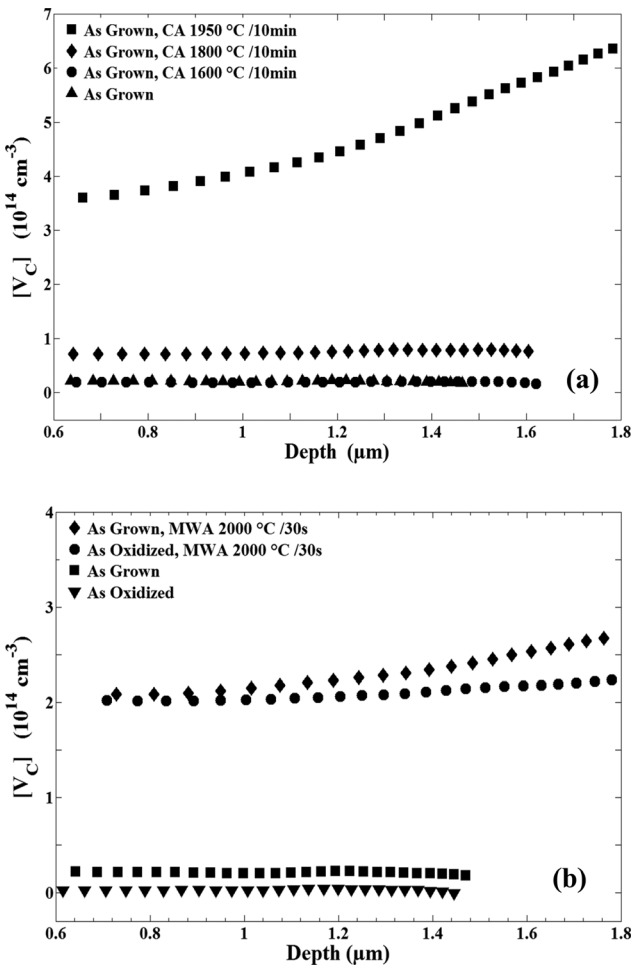

FIG. 6. Concentration-versus-depth profiles of V_C in (a) the as grown (group B) samples subjected to CA at different temperatures, and (b) the as grown (group B) and as oxidized (group C) samples subjected to MWA at 2000 °C.

bulk as the prevailing process and not Schottky formation at the surface with subsequent in-diffusion of V_C. The surface appears to act as a sink for migrating V_C's and/or to promote enhanced annihilation through reaction with C_I's. In addition, despite a rapid cooling rate uniform quenching of the samples may not hold fully and $[V_C]$ in the proximity of the surface may reflect a lower temperature than the annealing one, especially when approaching 2000 °C. Further studies are in progress to unveil the influence of the cooling rate on the depth distribution of $[V_C]$ and in fact, this rate may play a key role for optimizing the charge carrier lifetime, controlled by V_C, while maintaining a high efficiency of dopant activation during CA and MWA of ion-implanted layers.

IV. CONCLUSIONS

V_C in 4H-SiC is shown to have a single donor state (the EH_7 level) and a double acceptor state (the $Z_{1/2}$ level) in the upper part of the bandgap. $[V_C]$ increases rapidly with temperature after CA in the range 1600–1950 °C and for as oxidized samples (group C), which have a low initial concentration of V_C, the increase approaches three orders of magnitude. The data obey a close Arrhenius behaviour yielding a formation enthalpy of 5.0 ± 0.2 eV and an entropy factor ΔS of $\sim 5\ k$. The ΔS value implies substantial lattice relaxation around V_C, corroborating theoretical results in the literature showing that the surrounding Si atoms form re-constructed bonds causing symmetry lowering of V_C. MWA gives rise to lower $[V_C]$ than CA for comparable temperatures around 2000 °C, most likely due to the difference in duration (30 s versus 10 min) and indicating that steady-state conditions do not apply for the MWA. Hence, MWA may possibly be regarded as superior to CA for high-temperature device processing, resulting in longer minority charge carrier lifetime because of the lower $[V_C]$ and similar (or better) efficiency for dopant activation of high-fluence ion-implanted layers. However, no definite conclusion on CA versus MWA can be made at this stage and deeper understanding of the mechanism(s) controlling the V_C formation needs to be developed. Depth profiles of $[V_C]$ suggest formation in the bulk as the predominant process with a decreasing concentration in the proximity of the surface, and further studies are being pursued to unveil the role of different processing conditions, e.g., the cooling rate, on the distribution of $[V_C]$.

ACKNOWLEDGMENTS

Fruitful discussions and assistance by Dr. L. S. Løvlie during the initial stage of this study are highly appreciated. The collaboration with Professor Mulpuri V. Rao, Dr. Yong Lai-Tian, and Mr. Anindya Nath has been precious for the conduction of the microwave annealing experiments. Financial support by the Norwegian Research Council (FRINATEK program, WEDD project) is gratefully acknowledged.

[1]W. J. Choyke, H. Matsunami, and G. Pensl, *Silicon Carbide: Recent Major Advances, Springer Series: Advanced Texts in Physics* (Springer-Verlag, Berlin, 2004).
[2]T. Kimoto, A. Itoh, H. Matsunami, S. Sridhara, L. L. Clemen, R. P. Devaty, W. J. Choyke, T. Dalibor, C. Peppermüller, and G. Pensl, Appl. Phys. Lett. **67**, 2833 (1995).
[3]T. Dalibor, G. Pensl, T. Kimoto, H. Matsunami, S. Sridhara, R. T. Devaty, and W. J. Choyke, Diamond Relat. Mater. **6**, 1333 (1997).
[4]C. G. Hemmingsson, N. T. Son, O. Kordina, E. Janzén, J. L. Lindström, S. Savage, and N. Nordell, J. Appl. Phys. **81**, 6155 (1997).
[5]J. P. Doyle, M. K. Linnarsson, P. Pellegrino, N. Keskitalo, B. G. Svensson, A. Schöner, N. Nordell, and J. L. Lindström, J. Appl. Phys. **84**, 1354 (1998).
[6]C. G. Hemmingsson, N. T. Son, O. Kordina, A. Ellison, J. Zhang, and E. Janzén, Phys. Rev. B **58**, R10119 (1998).
[7]T. Hiyoshi and T. Kimoto, Appl. Phys. Express **2**, 41101 (2009); T. Hiyoshi and T. Kimoto, *ibid.* **2**, 91101 (2009).
[8]L. S. Løvlie and B. G. Svensson, Appl. Phys. Lett. **98**, 052108 (2011); Phys. Rev. B **86**, 075205 (2012).
[9]G. Alfieri, E. V. Monakhov, B. G. Svensson, and M. K. Linnarsson, J. Appl. Phys. **98**, 043518 (2005).
[10]B. Zippelius, J. Suda, and T. Kimoto, Mater. Sci. Forum **717–720**, 247 (2012).
[11]N. T. Son, X. T. Trinh, L. S. Løvlie, B. G. Svensson, K. Kawahara, J. Suda, T. Kimoto, T. Umeda, J. Isoya, T. Makino, T. Ohshima, and E. Janzén, Phys. Rev. Lett. **109**, 187603 (2012).
[12]R. Nipoti, R. Scaburri, A. Hallén, and A. Parisini, J. Mater. Res. **28**, 17 (2013).
[13]R. Nipoti, A. Nath, M. V. Rao, A. Hallén, A. Carnera, and Y.-L. Tian, Appl. Phys. Express **4**, 111301 (2011).
[14]J. M. Bluet, J. Pernot, J. Camassel, S. Contreras, J. L. Robert, J. F. Michaud, and T. Billon, J. Appl. Phys. **88**, 1971 (2000).
[15]Y. Negoro, T. Kimoto, H. Matsunami, F. Schmid, and G. Pensl, J. Appl. Phys. **96**, 4916 (2004).
[16]M. K. Linnarsson, M. S. Janson, U. Zimmermann, B. G. Svensson, P. O. Å. Persson, L. Hultman, J. Wong-Leung, S. Karlsson, A. Schöner, H. Bleichner, and E. Olsson, Appl. Phys. Lett. **79**, 2016 (2001).
[17]S. G. Sundaresan, M. V. Rao, Y.-L. Tian, M. Ridgway, J. A. Schreifels, and J. Kopanski, J. Appl. Phys. **101**, 073708 (2007).
[18]T. Kimoto, G. Feng, T. Hiyoshi, K. Kawahara, M. Noborio, and J. Suda, Mater. Sci. Forum **645–648**, 645 (2010).
[19]J. Wong-Leung, M. S. Janson, and B. G. Svensson, J. Appl. Phys. **93**, 8914 (2003).
[20]Y.-L. Tian, MRS Bull. **35**, 181 (2010).
[21]B. G. Svensson, K.-H. Rydén, and B. M. S. Lewerentz, J. Appl. Phys. **66**, 1699 (1989).
[22]L. Storasta, J. P. Bergman, E. Janzén, and A. Henry, J. Appl. Phys. **96**, 4909 (2004).
[23]K. Danno and T. Kimoto, J. Appl. Phys. **100**, 113728 (2006).
[24]J. Wong-Leung and B. G. Svensson, Appl. Phys. Lett. **92**, 142105 (2008).
[25]G. Alfieri and T. Kimoto, Mater. Sci. Forum **740–742**, 645 (2013).
[26]J. P. Biersack and L. G. Haggmark, *Nucl. Instrum. Methods* 174, 257 (1980); J. F. Ziegler, J. P. Biersack, and U. Littmark, in *The Stopping and Range of Ions in Solids*, edited by J. F. Ziegler (Pergamon, New York, 1985), Vol. 1.
[27]B. G. Svensson, C. Jagadish, A. Hallén, and J. Lalita, Phys. Rev. B **55**, 10498 (1997).
[28]L. C. Kimerling, J. Appl. Phys. **45**, 1839 (1974).
[29]L. S. Løvlie and B. G. Svensson, "Identification of acceptor- and donor-like deep states in SiC using non-uniform defect-versus-depth distributions" (to be published).
[30]E. V. Monakhov, J. Wong-Leung, A. Y. Kuznetsov, C. Jagadish, and B. G. Svensson, Phys. Rev. B **65**, 245201 (2002).
[31]S. B. Zhang and J. E. Northrup, Phys. Rev. Lett. **67**, 2339 (1991).
[32]A. Zywietz, J. Furthmüller, and F. Bechstedt, Phys. Rev. B **59**, 15166 (1999).
[33]L. Torpo, M. Marlo, T. E. M. Staab, and R. M. Nieminen, J. Phys. Condens. Matter **13**, 6203 (2001).
[34]M. Bockstedte, A. Mattausch, and O. Pankratov, Phys. Rev. B **68**, 205201 (2003).
[35]T. Hornos, A. Gali, and B. G. Svensson, Mater. Sci. Forum **679–680**, 261 (2011).
[36]T. Kimoto, private communication (2013).